Fabrication and Structural Observation of Molybdenum and Indium Nanocrystals Deposited on Si (111) Thin Films by UHV-FE-TEM

Miyoko TANAKA+, Masaki TAKEGUCHI* and Kazuo FURUYA

National Research Institute for Metals, 3-13 Sakura, Tsukuba 305-0003, JAPAN
**JEOL LTD., 3-1-2 Musashino, Akishima, Tokyo 196-8558, JAPAN*
+Phone: +81-298-59-5053, FAX: +81-298-59-5054, e-mail: iron @ nrim. go. jp

(Received: 18 February 1998; accepted: 20 February 1998)

Abstract:

Fabrication and structural observation of Mo and In nanoparticles deposited on Si (111) substrate was performed with an ultrahigh vacuum field emission transmission electron microscope (UHV-FE-TEM). High-resolution electron microscopy (HRTEM) of deposited Mo suggests the formation of nanocrystals with size of 2-3 nm. Some of them have twin boundaries inside. Dynamic observation of In deposition shows the formation of nanocrystals with various sizes. Nanocrystals more than 6 nm in size have tetragonal structure similar to bulk one and contains twin boundaries and stacking faults inside. About 2 nm-sized nanocrystal seems to have a fcc structure. Its shape fluctuates in a very short time scale within one second, sometimes showing coexistence of solid and liquid.

1. Introduction

Understanding the structure and the property of small particles is a fascinating subject because they do not behave like bulk materials and reveal unique and remarkable behavior. It is also important in nano-technology field such as for quantum dots. Various researchers have tried to fabricate and examine small particles with X-ray and electron diffraction [1], scanning tunneling microscopy (STM) [2] and transmission electron microscopy (TEM) [3]. Ultrahigh vacuum TEM (UHV-TEM) has especially clarified structures of nano-particles on surfaces by reflection, profile and plan view modes [4,5]. Since TEM images present structural information along the transmitted beam direction, it can be used not only to observe small particles and clusters but also to solve atomic details of surfaces, subsurface layers and buried interfaces [6,7].

By applying a field emission gun (FEG) to the TEM, more detailed information related to the surface structure will be acquired. The FEG has small energy spread and high coherency, so that it enables high-resolution and high-contrast TEM imaging and high-energy resolution chemical analysis with electron energy loss spectroscopy (EELS). A nanometric probe with large current is best for elemental analysis of small particle with spatial resolution with energy dispersive X-ray spectroscopy (EDS) [8].

An ultrahigh vacuum field emission transmission electron microscope (UHV-FE-TEM) has been developed for in-situ fabrication of nanoparticles and evaluation of the structures and electric properties [9]. UHV provides clean environment and therefore uncontaminated nanoparticles. Attached EDS and EELS systems are compatible with UHV conditions. In this study, Mo and In nanocrystals were deposited on Si (111) TEM samples and have been investigated with UHV-FE-TEM. HRTEM was performed with Mo nanocrystals deposited by electron beam evaporator and dynamic observation of In nanocrystals during deposition by thermal heater was carried out.

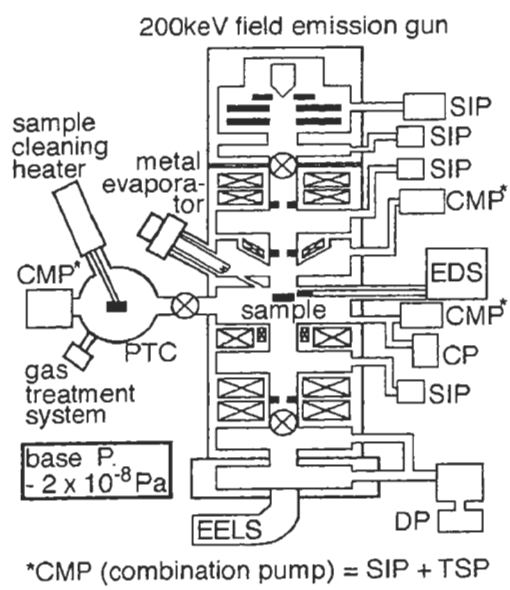

Fig.1 Schematic diagram of the analytical UHV-FE-TEM (JEM-2000VF).

2. Instrument and Experiment

Fig. 1 shows a schematic diagram of UHV-FE-TEM (JEOL-2000VF). Its point resolution at scherzer defocus is 0.21 nm and lattice resolution at information limit is 0.1 nm. It has a ZrO/W Schottky-type thermal FEG that provides large probe current density of 10^5 A/cm^2 and small energy spread of 0.7 eV at the electron source. Eight sputter ion pumps (SIPs), three titanium sublimation pumps (TSPs) and a cryo pump (CP) evacuate the TEM column. All lens systems are sealed by metal o-rings to be baked at up to 423 K. The combination of baking and differential pumping leads the vacuum level of the column to less than 2.0 x 10^{-8} Pa. Mass spectroscopy of residual gases indicates that the main residual gas is hydrogen.

Two evaporators are attached to the column in order to perform in situ evaporation of various kinds of metals. One is an electron beam evaporator and the other is a thermal heating evaporator. In the pre-treatment chamber (PTC) attached to the column, sample cleaning, gas treatment and metal deposition by another electron beam evaporator can be carried out separately with HRTEM. This chamber is kept at the same vacuum level as the column. The column is equipped with EDS and EELS apparatus.

Samples were cut from B doped p-Si (111) wafers (2-6 ohm·cm) and were prepared to TEM specimens by chemical etching, with etchant H_3PO_4: HNO_3: HF: CH_3COOH = 4:3:2:1. Electron beam (EB) deposition of Mo was carried out in the pre-treatment chamber. The amount of deposited Mo could not be measured during the deposition process in the present study, but the layer of Mo is estimated from HRTEM images to be about 2-3 nm. The deposition rate is calculated to be about 3-5 x 10^{-3}nm/s. Thermal deposition of In was carried out in the TEM column during observation. A TV-rate video camera provides dynamic observation of deposition process.

3. Results and Discussion

Fig. 2a shows a HRTEM micrograph of as prepared Si (111) sample after the EB deposition of Mo. The dominant lattice fringes of Si-substrate were deleted by tilting a specimen several degrees against [111] zone axis and defocusing with respect to selected diffraction spots of Si <220>. These procedures produced clear images of Mo nanocrystals

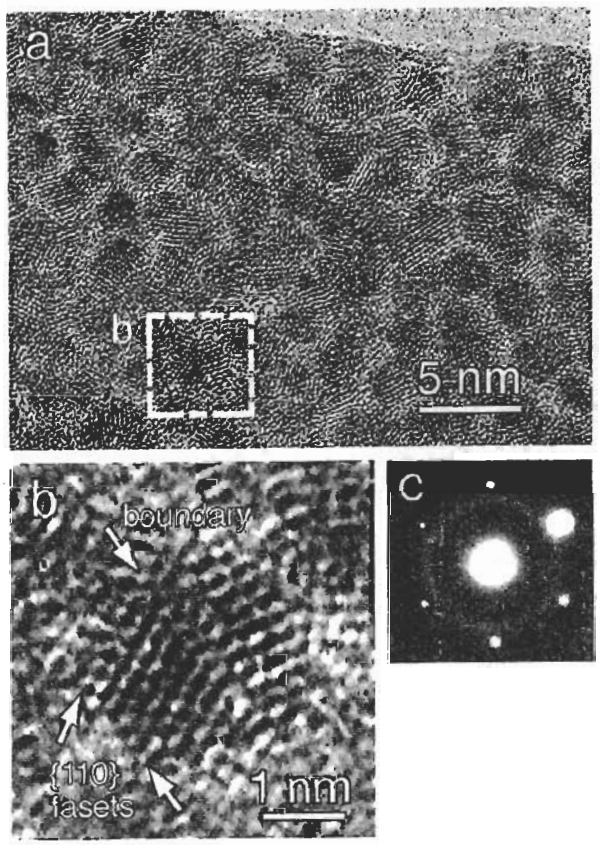

Fig.2 A TEM micrograph of Mo-nanocrystals deposited on Si (111) sample. a) A HRTEM image showing many Mo nanocrystals, b) a magnified image of a nanocrystal, b) its selected area diffraction (SAD) pattern.

with a mean size of about 2-3 nm but randomly oriented or twinned, which may imply the formation of multiply twinned particles (MTP's) [10]. The lattice fringes of the particles in magnified image in Fig. 2b indicate a detailed crystal structure. The existence of low angle boundaries in the particle implies polycrystalline structure in a nanocrystal. As Mo has a bcc structure with lattice parameter a = 0.315 nm, the left part of the crystal seems to have two {110} facets and with [111] beam incidence. The right part of the crystal seems to have (100) plane with {110} facet and {110} boundary, but the exact morphology is difficult to know because of the tilting of the substrate for imaging of such a small particle. Selected area diffraction (SAD) in Fig. 2c shows Mo <110> Debye ring with a certain width, because of the smallness and random orientation of the nanocrystals. The lattice spacing in Fig. 2b shows an agreement with the spacing calculated from the Mo <110> Debye ring.

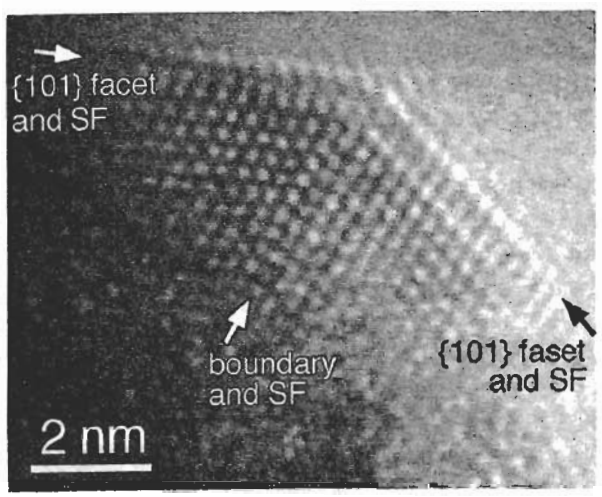

Fig.3 TEM micrograph of that larger In-nanocrystal deposited on Si (111) sample which seems to have tetragonal structure. Twin boundary and stacking faults are revealed. The image is recorded via videotape during the deposition process.

Deposition of Indium on Si (111) was performed in TEM column during observation. Fig. 3 shows a still image of deposited nanocrystal grabbed from videotape. It stays at the edge of the sample, forming about 6 nm-sized nanocrystal. From the lattice spacing measurement after the image processing based on fast Fourier transformation (FFT), it turned out to have a tetragonal structure with [111] beam incidence. The crystal structure of bulk In is body centered tetragonal (bct) with lattice parameters a = 0.325 nm and c= 0.495 nm. This nanocrystal has almost the same parameters. Since small particle should have minimum energy shape (Wulff construction) [11,12], this crystal has two {101} facets which have minimum surface energy. It also contains twin boundaries at the center and stacking faults (SFs) at the boundary and near the surface. The existence of twin boundary contributes to decrease in energy [13,14], but in this case high internal strain may cause stacking fault at the twin in addition to the formation of boundary.

Smaller nanocrystals were also observed during the deposition process. Fig. 4 shows sequential images of a nanocrystal with size of about 2 nm, also grabbed from videotape. The time difference between each image is about 0.2 sec. Frequent changes in the morphology are observed. These are considered to occur by deposition of In and electron beam irradiation. In all images, the crystal structure seems to be fcc structure with [110] beam incidence. The lattice parameter change in small particles was observed in the previous works [15,16]. As the lattice size decreases, the effect of the surface stress increases in the total surface free energy [17]. Thus the lattice tries to change its lattice parameter to reduce the total energy by reducing an elastic strain of the surface and balancing it with an increase of internal strain. Previous study has reported that bulk tetragonal structure of In changes into fcc structure near the cluster size of 5 nm [18]. Present results support this tendency by forming closed-pack structure for smaller particles to release the strain.

Although the exact three-dimensional structure of the crystal is not known, each image seems to show {111} facets. In Fig. 4a, the crystal

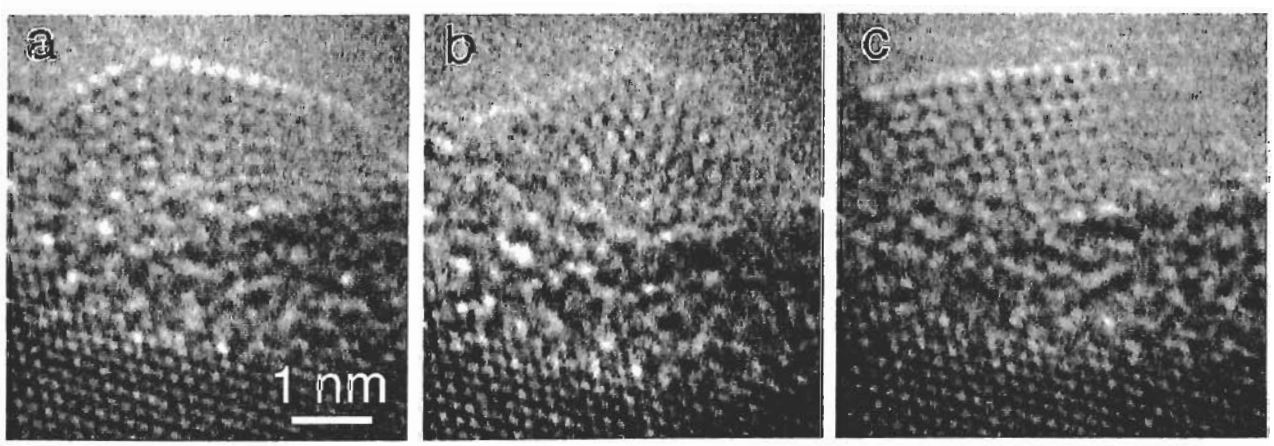

Fig.4 Sequential images of smaller In-nanocrystal fluctuating its structure. This time crystal structure seems like fcc one. a) With twin and liquid-like phase, b) with only twin and c) coexistence of solid-liquid states.

shows twin boundary in left part. Even in this size range, twin boundary is preferable to minimize the crystal energy. Another interesting phenomena emerges in the right end of this crystal, which transforms to liquid or amorphous state. This transition also happens in the image in Fig. 4c. In some cases, all part of a crystal does not show any lattice fringes but with a hemispherical shape which is considered to be melting. In Fig. 4b, the crystal shows twin boundary similar to a crystal in Fig. 3. As mentioned above, the transition from Fig. 4a to Fig. 4b and 4c occurred in a very short time. Since the melting point of In is 430 K and the depressed melting point of small particle should be lower [19], the local temperature raise by electron beam irradiation and the deposition of In may cause both fast structural transformations and coexistence of solid and liquid state.

This "fluctuating structure" phenomenon is well observed in fcc metals [20]. It has been reported that electron beam heating is not enough to raise the temperature near to the melting point and that the fluctuation can be explained in terms of potential energy surface [21]. The temperature at which the thermal fluctuation is large enough to overcome the potential energy barriers is thought to be lower than the melting point and above this temperature the particles are able to constantly change their shape in quasi-molten phase. The temperature required for this transition becomes lower as the particle size gets smaller [10]. Furthermore, atom addition to the crystal due to the deposition of In can change the height of potential barriers. This may explain the present result that shows frequent transition in 2 nm-sized crystal but rather slow transformation in larger crystal.

4. Summary

Fabrication and structural observation of Mo and In nanoparticles deposited on Si (111) substrate was performed with UHV-FE-TEM. HRTEM of Mo nanoparticle suggests the formation of nanocrystals with size of 2-3 nm. Some of them have twin boundaries inside. SAD of these crystals shows the smallness and random orientation of the nanocrystals. Dynamic observation of In deposition shows the formation of nanocrystals with various sizes. Nanocrystals more than 6 nm in size have tetragonal structure similar to bulk one and contains twin boundaries and stacking faults inside. About 2 nm-sized nanocrystal seems to have a fcc structure. Surface strain may be the reason to cause this crystalline structural change. Its shape fluctuates in a very short time scale, sometimes showing coexistence of liquid and solid. This may be due to the electron beam heating which raise the system to a certain state where the particles prefer to change their structure.

References

1. J. B. Cohen, Ultramicroscopy **34**, 41 (1990)
2. A. Shibata and K. Takayanagi, Jpn. J. Appl. Phys. **32**, 1385 (1993)
3. A. Howie, L. D. Marks and S. J. Pennycook, Ultramicroscopy **8**, 163 (1982)
4. M. Mitome and K. Takayanagi, Surf. Sci. **242**, 69 (1991)
5. N. Doraiswamy, G. Jayaram and L. D. Marks, Phys. Rev. B **51**, 10167 (1995)
6. Y. Haga and K. Takayanagi, Ultramicroscopy **45**, 95 (1992)
7. E. Bengu, R. Plass, L. D. Marks, T. Ichihashi, P. M. Ajayan and S. Iijima, Phys. Rev. Lett. **77**, 4226 (1996)
8. Y. Yu, D. Ping, Y. Wang, J. Huang, D. Li and H. Ye, J. Surf. Anal. **3**, 203 (1997)
9. M. Tanaka, K. Furuya, M. Takeguchi and T. Honda, Thin Solid Films, to be published.
10. P. M. Ajayan and L. D. Marks, Phase Transitions **24**, 229 (1990)
11. G. Wulff, Zeits. F. Kristallog **34**, 449 (1901)
12. L. Wang, L. M. Falicov and A. W. Searcy, Surf. Sci. **143**, 609 (1984)
13. L. D. Marks, Phil. Mag. A 49, 81 (1984)
14. C. Cleveland and U. Landman, J. Chem. Phys. **94**, 7376 (1991)
15. M. Multani, P. Ayyub, V. Palkar and P. Guptasarma, Phase Transitions **24**, 91 (1990)
16. S. Onodera, J. Phys. Soc. Japan **61**, 2191 (1992)
17. D. Wolff, Surf. Sci. **226**, 1990 (1990)
18. A. Yokozeki and G. D. Stein, J. Appl. Phys. **49**, 2224 (1978)
19. R. Cofman, P. Cheyssac and R. Garrigos, Phase Transitions **24**, 283 (1990)
20. S. Iijima and T. Ichihashi, Phys. Rev. Lett. **56**, 616 (1986)
21. L. D. Marks, Rep. Prog. Phys. **57**, 603 (1994)